Journal of Molecular Imaging & Dynamics

ISSN: 2155-9937

Sanjeev et al., J Mol Imag Dynamic 2017, 7:1
DOI: 10.4172/2155-9937.1000132

Research Article OMICS International

Effect of C-Terminal Truncations on the Aggregation Propensity of Alpha-Synuclein - A Potential of Mean Force Study

Airy Sanjeev and Venkata Satish Kumar Mattaparthi*

Molecular Modelling and Simulation Laboratory, Department of Molecular Biology and Biotechnology, Tezpur University, Tezpur-784 028, Assam, India

***Corresponding author:** Venkata Satish Kumar Mattaparthi, Molecular Modelling and Simulation Laboratory, Department of Molecular Biology and Biotechnology, Tezpur University, Tezpur-784 028, Assam, India, Tel: +91 08811806866; E-mail: mvenkatasatishkumar@gmail.com

Rec date: June 1, 2017; **Acc date:** June 27, 2017; **Pub date:** June 30, 2017

Abstract

α-Synuclein is an intrinsically disordered protein which has a prominent role in Parkinson's disease (PD). Several familial variants of α-synuclein have been reported to associate with inherited PD. Several studies have highlighted the presence and association of the C-terminus of truncated forms of α-synuclein with Wild type α-synuclein (WT α-syn) at much higher level in patients with Lewy body diseases and they are found to decrease the reductive capabilities and potentially results in permanent oxidation of α-synuclein. To understand the impact of C-terminal truncations on the aggregation propensity of WT α-syn, the inter-molecular interactions between them are critical. Here we demonstrate the interactions between the WT α-syn and its three C-terminal truncations 95 (α-syn 95), 120 (α-syn 120) and 123 (α-syn 123), using Molecular Dynamics Simulations and Potential of Mean Force study (PMF). From the PMF study, we observed C-terminal truncation 120 (α-syn 120) to bind strongly to WT α-syn than the other truncated forms of α-synuclein. We also noticed number of hydrogen bonds to be larger, high geometrical shape complementarity score, larger number of interface residues and interface area for the hetero-dimer (WT α-syn-α-syn 120) than other hetero-dimers (WT α-syn - α-syn 95/123). We therefore can infer that among α-syn 95, α-syn 120 and α-syn 123, α-syn 120 to show more association with WT α-syn. This is because in α-syn 120, more amino acids have been removed in comparison to α-syn 123. In contrast, α-Syn 95 shows less interaction with WT α-syn because of the absence of the entire C-terminal region. Our findings suggest that more the truncation on the C-terminal region of α-synuclein more will the effect on its aggregation.

Keywords: Disordered; Parkinson's disease; Truncation; Molecular Dynamics; Potential of mean force

Introduction

α-Synuclein (α-syn) is a cellular acidic protein of 140 amino acid residues that release neurotransmitters in the presynaptic nerve terminals [1-4] and whose abnormal aggregation results at the onset of Parkinson's disease (PD) [5-9]. Accumulation of α-syn fibrils in neuronal inclusions is the major pathological process involved in PD. PD is a neuro-degenerative disorder, sporadically affecting nearly 10 million people around the world and associated with common ageing of a person [8,10-14]. It is considered to be a progressive and movement disorder which results in slow movement and develops cardinal symptoms such as tremor, bradykinesia, rigidity and postural instability [15]. There are also various other motor symptoms associated with PD such as freezing of gait, altered gait pattern, and motor co-ordination deficits [16,17]. Apart from that, some non-motor symptoms are also observed to be associated with PD which is anxiety and depression [18,19]. Hence in general, PD shows a direct link with mobility and motor control. Aggregation of α-syn as Lewy Neurites (LN) or Lewy Bodies (LB) is a pathological demonstration for dementia in both PD and DLB (Dementia in Lewy Bodies) in cortical areas [20-22]. The mechanism underlying protein aggregation and corresponding neurochemical correlations are still not properly understood. α-Syn protein consists of three distinct structural and dynamical properties which includes a membrane binding N-terminal helical segment (1-60); an acidic C-terminal region, weakly associated with the membrane (95-140) and a hydrophobic central fibril core region (NAC: non-amyloid β component) (61-95) which acts as a sensor of lipid properties, determining the affinity of α-syn membrane binding [23-25]. The central region that includes the NAC fragment is involved in the mechanism of α-syn aggregation, and is reported to play a key role in modulating the affinity of α-syn for cellular membranes [26-32]. Studies reveal that NAC domain is partially protected by the charges present in the positive N-terminal and negative C-terminal regions [33]. However, α-syn possesses dynamic conformations that are stabilized by long-range interactions providing a substantial degree of compactness [33]. These interactions occur between NAC region and C-terminal region and also between N and C-terminal region due to the effect of electrostatic and hydrophobic contacts which might prevent aggregation [33]. It has also been reported that the NAC domain, that plays a significant role in α-syn aggregation propensity is likely to be included in the membrane-sensor region and also to have functional relevance [30,34,35]. The NAC domain has the capability for defining the affinity of α-syn with lipid membranes and also in modulating partition between the bound and free states of membrane in the synaptic terminal [36-40]. Indeed, it is evident from earlier reports that α-syn exists in a state of equilibrium *in vivo* between the membrane-bound and cytosolic states, with membrane partition tightly being regulated [23]. During the process of aggregation, these membrane interactions highlight the importance of the interaction between various functional states of α-syn and its aggregation mechanism leading to PD.

Though the function of native α-syn is not clear, but it has been shown that α-syn can regulate the transport of neurotransmitter-filled vesicle to the release zone and assembly of complexes in presynaptic protein [41,42]. α-syn form aggregates which later forms insoluble

intracellular filamentous inclusions called as LB or LN [20] that are the significant histo-pathological symptoms of PD. Though the mechanism leading to the fibrillation process of α-syn are not known properly, but alteration and truncation of the C-terminal region of α-syn was shown to induce the aggregation mechanism in several models. Among the various mechanisms that can promote the aggregation propensity of α-syn, C-terminal truncation in α-syn have been recognized as a promoter/enhancer for α-syn fibrillization and oligomerization [43-46]. It has been reported earlier that the C-terminal truncations decreases the reductive capabilities and can potentially results in permanent oxidation of α-syn [47]. Hence it was shown that C-terminal region of α-syn is required for protein stability as the truncation mutants present in α-syn might have a higher tendency to fibrillate [48-50]. Also, the C-terminal truncated forms have been observed to aggregate faster than the full length protein of α-syn [43,45]. The C-terminal region of α-syn plays a major part in the interaction of α-syn with other proteins and also with some small molecules [42,51-56]. The binding of important metals such as iron, copper and various other metals have been shown to influence the aggregation propensity of α-syn [14]. Consequently, inhibiting the α-syn C-terminal truncation might modify the period of disease in multiple system atrophy (MSA) and various other related neuro-pathogenesis [57] by reducing the α-syn aggregation and oligomerization process. Studies have shown that the carboxyl terminal truncation present in human α-syn was also observed in human DLB brain, and these truncations can increase α-syn propensity to aggregate *in vitro* [49,58]. Several evidences have been seen from literature which states that the missense mutations linked with PD can increase the proliferation of C-terminally truncated α-syn species. This type of truncations present in α-syn might occur in healthy brains too. Remarkably it has been observed that various truncated species might accelerate the fibrillation propensity of the full-length protein of α-syn both *in vivo* [59] and *in vitro* [46], and hence may contribute or initiate the aggregation process. The C-terminal region of α-syn is however less conserved than the N-terminal region which shows that interaction between these two regions helps to stabilize the conformations and protect it from various truncations and aggregation. The modifications done in C-terminal region may protect the various cleavage sites and also stabilize α-syn protein against proteolytically accessible conformations. As a result, the C-terminal truncation can generate production of toxic aggregates and hence promotes the neuro-degeneration process [43-45,60-70].

In order to understand the mechanism by which the C-terminal truncations affect the aggregation propensity of α-syn, the inter-molecular interactions between them might play a vital role. In this work, we demonstrate the interactions between the WT α-syn and its three important C-terminal truncations 95, 120 and 123, using Molecular Dynamics (MD) Simulation and Potential of Mean Force study (PMF) [70]. The starting structure of the individual hetero-dimer containing WT α-syn and one of its three important C-terminal truncations 95, 120 and 123 for PMF study were obtained from the PatchDock [71] online docking server and the structures were then refined using FireDock [72] server. The interacting residues between the monomeric units of the hetero-dimer of α-syn and C-terminal truncations (α-syn 95, 120 and 123) were analyzed using PDBSum online server [73]. Using this server, the various bonding and non-bonding interactions was studied. We also noticed number of hydrogen bonds to be larger, high geometrical shape complementarity score, larger number of interface residues and interface area for the hetero-dimer (WT α-syn - α-syn 120) than other hetero-dimers (WT α-syn - α-syn 95/123). From the PMF study, we observed C-terminal truncation 120 (α-syn 120) to bind strongly to WT α-syn than the other truncated forms of α-syn. Thus, we can infer that among α-syn 95, α-syn 120 and α-syn 123, α-syn 120 show more association with WT α-syn and can easily form a hetero-dimer and aggregate at a faster rate than the other C-terminal truncated form of α-syn. Our findings suggest that more the truncation on the C-terminal region of α-syn more will be its impact on the aggregation.

Methodology

Building the initial structures of the C-terminal truncated counter-parts of α-syn

The model structure of the three-truncated counter-parts of α-syn: C-terminal truncation 95 (α-syn 95), C-terminal truncation 120 (α-syn 120) and C-terminal truncation 123 (α-syn 123) (Figure 1) were prepared from the WT structure of α-syn with PDB ID: 1XQ8 taken from Protein Data Bank [74] by truncating the various residues present in C-terminal region using Pymol visualizing software (PyMOL Molecular Graphics System).

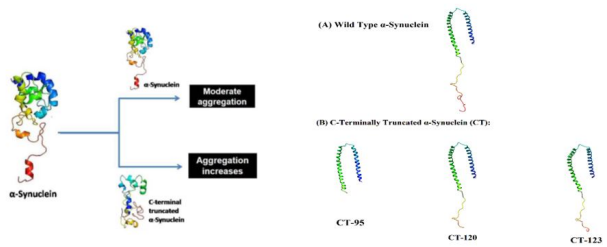

Figure 1: 3D structures of WT and the three truncated counter-parts of α-Synuclein (Syn-95/120/123) obtained using Chimera softwares.

Construction of dimer

Using the PatchDock [71] online docking server, we constructed the hetero-dimers (WT α-syn - α-syn 95, WT α-syn - α-syn 120, WT α-syn - α-syn 123) by docking the two corresponding monomeric units. PatchDock is a rigid docking server that is based on geometry docking algorithm [71] which finds the optimum candidate conformers and uses Root Mean Square Deviation (RMSD) clustering to eradicate the redundant solutions. Based on the atomic desolvation energy [75] as well as geometric fit, a particular score was given to the candidate solution. In our study, the RMSD value was taken as 4 Å as default value for clustering the solutions. For refining the conformers obtained from the PatchDock docking server, we used the FireDock server [72]. This server targets the flexibility problem and solutions scoring that are formed by fast rigid-body docking algorithms. It refines based on an energy function by spending 3.5 seconds per candidate solution from a total of 1000 potential docking candidates. Based on an energy function, the candidate model conformers were refined and scored in the server. The individual candidate solutions are refined by optimizing the side-chain conformations and also by rigid body orientation. This energy score consists of atomic contact energy (ACE), electrostatics,

hydrogen bonding, soften van der Waals interactions and estimation of binding free enegy.

Further to obtain the details about the various protein-protein interactions between the monomeric units of dimer of WT α-syn and the C-terminal truncated α-syn (α-syn 95/120/123) conformers, we used PDBSum online server. This server gives a brief illustration about the varying interacting residues, interfaces between the chains, overview of which chains interact with the other chain and interactions across any selected interface of the dimer complex of WT α-syn and C-terminal truncations.

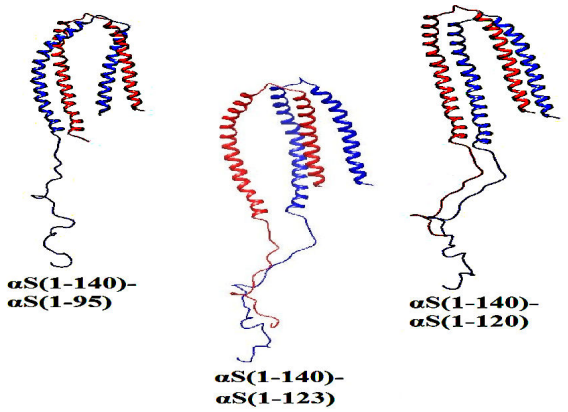

Figure 2: Dimer conformers of the three complex αS and C-terminal truncated 95 (Syn 95), αS and C-terminal truncated 120 (Syn 120) and αS and C-terminal truncated 123 (Syn 123) obtained from PatchDock server.

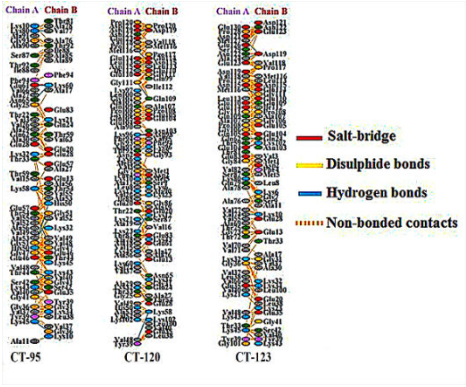

Figure 3: Residue-residue interactions of the hetero-dimer of αS and C-terminal truncated (Syn 95/120/123) showing the various bonded and non-bonded interactions like salt-bridge (red colour), disulphide bonds (yellow colour), hydrogen bonds (blue colour) and non-bonded contacts (orange colour) as predicted by PDBsum server.

The dimer conformer having the best geometric shape complementarity score, surface area, atomic contact energy (ACE) obtained from PatchDock (Figure 2) was submitted onto the PDBSum online server for inter-molecular interactions study (Figure 3). A detailed summary of the various bonded, non-bonded contacts and the interacting residues involved between the monomeric units of the dimer of WT α-syn and C-terminal truncations (α-syn 95/120/123) were obtained from this server.

Potential of mean force study

The conformer having best atomic contact energy (ACE) value, interface area and geometric complementary score obtained from PatchDock was subjected to energy minimization, heating and equilibration dynamics and then proceeded for PMF study. Using Weighted Histogram Analysis Method (WHAM) [76-78], we calculated the PMF of WT α-syn and C-terminal truncation (α-syn 95/120/123) conformers using the equilibrium umbrella sampling simulations. We used the umbrella sampling method [79] to calculate the free energy profiles of the corresponding dimers. In umbrella sampling, the exploration of phase space relies on MD simulations over a series of regions (windows) and they are distributed along a predefined reaction path. Around the selected regions of phase space, biasing potentials are added to Hamiltonian to confine the molecular system. The biasing potential is a harmonic potential [79] to keep the system near a specified value in the reaction path. This process is done for a number of windows along the reaction path. For every window, equilibrium simulations are carried out and biased probability distributions (histogram) are obtained. The WHAM is used to determine the optimal free energy constants for the combined simulations. To study the degree of association of monomeric units of WT α-syn and C-terminal truncation (α-syn 95/120/123) conformers, we carried out PMF computation by varying the distance between center of masses (COMs) of the two monomeric units between them in two opposite directions (increasing and decreasing). The PMF has been computed as a function of inter-chain distances between the two monomeric units of the dimer complexes. The "inter-chain distance" is the distance between COM of the two monomers. Thereby, umbrella samplings were performed with reaction coordinate as the distance between the monomeric units for WT α-syn and C-terminal truncation (α-syn 95/120/123) conformers. By performing COM distance with constrained MD simulations, initial configurations were generated for the series of umbrella sampling MD simulation in WT α-syn and C-terminal truncation (α-syn 95/120/123) conformers. Distance between the COMs of the monomeric units of the dimer present in WT α-syn and C-terminal truncation (α-syn 95/120/123) was changed with time from 4 to 40 Å spanning different configurations. Initial configurations were extracted as a grid of spacing 15 Å for WT α-syn - α-syn 120, 24 Å for WT α-syn - α-syn 95 and 30 Å for WT α-syn - α-syn 123.

Results and Discussion

Secondary structure analysis for the C-terminal truncated conformers

The secondary structure analysis for the C-terminal truncated conformers were carried out using online server Self-Optimized Prediction from Multiple Alignment (SOPMA). This server uses the homologue method by taking the short homologous sequence of amino acids that tend to form similar secondary structures. This database merely consists of 126 chains of non-homologous proteins. From the analysis of secondary structure contents, we noticed α-syn 95 to have higher number of extended strand and beta turns (Table 1). From Table 1, we observed that the helical and strand contents are more in α-syn 95 whereas the coil content is more in α-syn 120 and α-

syn 123. Hence, we can infer that C-terminally truncated counterparts might play an important role in the aggregation propensity as it contains the necessary secondary structural contents for fibrillation of α-syn.

Secondary Contents	Percentage (%)		
	αS95	αS120	αS123
Alpha helix	65.26	58.33	53.66
Extended strand	14.74	1s0.83	13.82
Beta turn	12.63	10	11.38
Random coil	7.37	20.83	21.14
Bend bridge	0	0	0

Table 1: Secondary Structure details of the truncated conformers of αS95, αS120 and αS123 monomers showing the percentage of secondary contents, graph and similarity threshold as predicted by SOPMA (Self-Optimized Prediction Method with Alignment).

Dimer study

To study the docking conformations for the corresponding hetero-dimer of WT α-syn and C-terminal truncation (α-syn 95/120/123) of synuclein, we built the model hetero-dimer complex structures using the PatchDock online server. From the PatchDock server, the complex structure of hetero-dimer of WT α-syn and C-terminal truncation (α-syn 95/120/123) conformers having the best ACE value, interface area and geometrical shape complementarity score was obtained (Figure 2). From our results, we noticed that WT α-syn interacts with α-syn 95 with a geometric shape complementarity score of 12154, approximate interface area of 3054.60 Å2 and atomic contact energy (ACE) of -563.83 kcal/mol. In the same manner, we observed that WT α-syn interacts with α-syn 120 with a geometric shape complementarity score of 20950, approximate interface area of 4043.30 Å2 and atomic contact energy (ACE) of -840.07 kcal/mol whereas WT α-syn interacts with α-syn 123 with a geometric score of 16995, approximate interface area of 3883.00 Å2 and atomic contact energy (ACE) of -460.85 kcal/mol respectively. The complex dimer structures obtained from PatchDock were refined using FireDock online server that are ranked based on Global energy, ACE value, Attractive van der Waals, Repulsive van der Waals and Hydrogen Bond.

We analyzed the interacting residues and the interface area for the complex model structure of WT α-syn and C-terminal truncation (α-syn 95/120/123) hetero-dimer having maximum interface area using the PDBSum online server. From this server, the interface and possible interacting residues across the interface were obtained. The results for the PDBSum were summarized in Table 2. From Table 2, we noticed the total number of interface residues in WT α-syn and α-syn 95 complex was found to be 95 and the interface area for each monomeric unit involved in the interaction was observed to be more than 2238 Å2. While in the case of WT α-syn and α-syn 120 complex we observed the total number of interface residues to be 122 and the interface area to be more than 2880 Å2. Similarly, for WT α-syn and α-syn 123 complex, we noticed the total number of interface residues to be 110 and the interface area to be more than 2543 Å2.

We observed that all the three-complex hetero-dimer structures WT α-syn and C-terminal truncation (α-syn 95/120/123) were stabilized by molecular interactions like hydrogen bonding, salt-bridges and non-bonded contacts (Figure 3). From the Table 2, we noticed the number of hydrogen bonds to be more in WT α-syn and α-syn 95 (11) and WT α-syn and α-syn 120 (11) complex than in the WT α-syn and α-syn 123 (7) complex. Among the C-terminal truncated conformers α-syn 95, α-syn 120 and α-syn 123, we observed α-syn 120 show more association with WT α-syn. This is because in α-syn 120, more amino acids have been removed in comparison to α-syn 123. However, α-syn 95 shows less interaction with WT α-syn because of the absence of the entire C-terminal region.

Dimer	Chain	Number of interface residues	Interface area (Å2)	Number of salt bridges	Number of disulphide bonds	Number of hydrogen bonds	Number of Non-bonded contacts
αS (1-140)-αS (1-95)	A	48	2325	2	-	11	1086
	B	47	2236				
αS (1-140)-αS (1-120)	A	66	2881	2	-	11	1299
	B	56	3051				
αS (1-140)-αS (1-123)	A	58	2628	2	-	11	1692
	B	52	2544				

Table 2: Interface plot statistics of αS (1-140)-αS (1-95), αS (1-1s40)-αS (1-120) and αS (1-140)-αS (1-123) showing the total number of interface residues, interface area, number of salt bridge and total non-bonded contacts.

For this reason, we can suggest that there is a strong inter-molecular interaction between the WT α-syn and C-terminal truncated α-syn (95/120/123) that can accelerate the aggregation propensity and form dimer easily.

Computation of potential of mean force

To carry out the association study of WT α-syn and C-terminal truncated α-syn (95/120/123) hetero-dimer complexes, we have combined MD simulation along with umbrella sampling methodology [79] to examine the various interactions between WT α-syn and C-terminal truncated α-syn (95/120/123) hetero-dimer in terms of PMF. The PMF for WT α-syn and C-terminal truncated α-syn (95/120/123)

hetero-dimer interaction in water at room temperature as a function of reaction co-ordinate is shown in Figure 4. We defined the reaction co-ordinate as the distance between the COMs of the synuclein monomeric units. From Figure 4, we see presence of a minimum of WT α-syn and α-syn 95 at a separation of 24 Å with a barrier to dissociation of 1.3 kcal/mol. From the association of WT α-syn and α-syn 120 and 123, we found the presence of a minimum at a separation of 15 Å and 30 Å with a barrier to dissociation of 2.5 and 1.5 kcal/mol respectively. We thus noticed that the energy barrier for the WT α-syn and α-syn 120 was larger when compared to WT α-syn and α-syn 95 and WT α-syn and α-syn 123. Hence, we observed a predominant transient interaction between WT α-syn and α-syn 120 that can be further used to understand the fibrillation propensity. Our observations suggest that WT α-syn and α-syn 120 can easily form a dimer and can aggregate at a faster rate than the corresponding hetero-dimer complex.

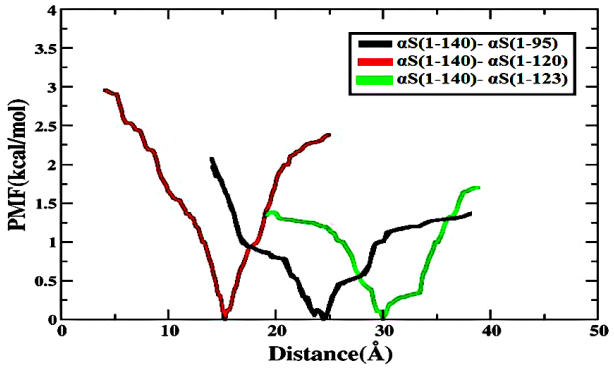

Figure 4: PMF plot for the hetero-dimer of αS and C-terminal truncated (Syn 95/120/123) showing the varying optimal distance and the attractive and repulsive forces that are holding the dimers.

Conclusion

In this study, we have investigated the inter-molecular interactions between the WT α-syn and C-terminal truncation (α-syn 95/120/123) to understand the mechanism by which it affects the aggregation propensity of α-syn using the PMF study. We compared the association of WT α-syn with its C-terminal truncation (α-syn 95/120/123). From the PMF study, we observed C-terminal truncation 120 (α-syn 120) to bind strongly to WT α-syn than the other truncated forms of α-syn. We also noticed number of hydrogen bonds to be larger, high geometrical shape complementarity score, larger number of interface residues and interface area for the hetero-dimer (WT α-syn - α-syn 120) than other hetero-dimers (WT α-syn - α-syn 95/123). Thus, we can infer that among α-syn 95, α-syn 120 and α-syn 123, α-syn 120 show more association with WT α-syn. Our findings suggest that more the truncation on the C-terminal region of α-syn more will the effect on its aggregation.

Acknowledgements

We thank the Tezpur University and UGC for the start-up grant. We also thank the DBT funded Bioinformatics Infrastructure facility in the Department of Molecular Biology and Biotechnology at Tezpur University for providing us computational facility for carrying out this research work.

References

1. Auluck PK, Caraveo G, Lindquist S (2010) α-Synuclein: membrane interactions and toxicity in Parkinson's disease. Annu Rev Cell Dev Biol 26: 211-33.
2. Cooper AA, Gitler AD, Cashikar A, Haynes CM, Hill KJ, et al. (2006) Alpha-synuclein blocks ER-Golgi traffic and Rab1 rescues neuron loss in Parkinson's models. Science 313: 324-328.
3. Vargas KJ, Makani S, Davis T, Westphal CH, Castillo PE, et al. (2014) Synucleins Regulate the Kinetics of Synaptic Vesicle Endocytosis. J Neurosci 34: 9364–9376.
4. Soper JH, Roy S, Stieber A, Lee E, Wilson RB, et al. (2008) Alpha-synuclein-induced aggregation of cytoplasmic vesicles in Saccharomyces cerevisiae. Mol Biol Cell 19: 1093-1103.
5. Luk KC, Kehm VM, Zhang B, O'Brien P, Trojanowski JQ, et al. (2012) Intracerebral inoculation of pathological α-synuclein initiates a rapidly progressive neurodegenerative α-synucleinopathy in mice. J Exp Med 209: 975-986.
6. Dobson CM (2003) Protein folding and misfolding. Nature 426: 884-890.
7. Uversky VN, Eliezer D (2009) Biophysics of Parkinson's disease: structure and aggregation of alpha-synuclein. Curr Protein Pept Sci 10: 483-499.
8. Chiti F, Dobson C (2006) Protein Misfolding, Functional Amyloid, and Human Disease. Annu Rev Biochem 75: 333-366.
9. Luth ES, Stavrovskaya IG, Bartels T, Kristal BS, Selkoe DJ (2014) Soluble, prefibrillar α-synuclein oligomers promote complex i-dependent, Ca^{2+}-induced mitochondrial dysfunction. J Bio Chem 289: 21490-21507.
10. Bodner RA, Outeiro TF, Altmann S, Maxwell MM, Cho SH, et al. (2006) Pharmacological promotion of inclusion formation: a therapeutic approach for Huntington's and Parkinson's diseases. Proc Natl Acad Sci USA 103: 4246-4251.
11. Perrin RJ, Woods WS, Clayton DF, George JM (2000) Interaction of human alpha-Synuclein and Parkinson's disease variants with phospholipids. Structural analysis using site-directed mutagenesis. J Biol Chem 275: 34393–34398.
12. Comellas G, Lemkau LR, Zhou DH, George JM, Rienstra CM (2012) Unique structural intermediates during alpha-synuclein fibrillogenesis on phospholipid vesicles. J Am Chem Soc 134: 5090-5099.
13. Breydo L, Wu JW, Uversky VN (2012) A-synuclein misfolding and Parkinson's disease. Biochim Biophys Acta 1822: 261-285.
14. Uversky VN, Li J, Fink AL (2001) Evidence for a partially folded intermediate in alpha-synuclein fibril formation. J Biol Chem 276: 10737-10744.
15. Ramirez EP, Vonsattel JP (2014) Neuropathologic changes of multiple system atrophy and diffuse Lewy body disease. Semin Neurol 34: 210-216.
16. Jankovic J (2008) Parkinson's disease: clinical features and diagnosis. J Neurol Neurosurg Psychiatry 79: 368-376.
17. Bartels AL, Leenders KL (2009) Parkinson's disease: the syndrome, the pathogenesis and pathophysiology. Cortex 45: 915-921.
18. Gjerstad MD, Wentzel-Larsen T, Aarsland D, Larsen JP (2007) Insomnia in Parkinson's disease: frequency and progression over time. J Neurol Neurosurg Psychiatry 78: 476-479.
19. Walsh K, Bennett G (2001) Parkinson's disease and anxiety. Postgrad Med J 77: 89-93.
20. Spillantini MG, Schmidt ML, Lee VM, Trojanowski JQ, Jakes R, et al. (1997) Alpha-synuclein in Lewy bodies. Nature 388: 839-840.
21. Wakabayashi K, Matsumoto K, Takayama K, Yoshimoto M, Takahashi H (1997) NACP, a presynaptic protein, immunoreactivity in Lewy bodies in Parkinson's disease. Neurosci. Lett 239: 45-48.
22. Baba M, Nakajo S, Tu PH, Tomita T, Nakaya K, et al. (1998). Aggregation of alpha-synuclein in Lewy bodies of sporadic Parkinson's disease and dementia with Lewy bodies. Am J Pathol 152: 879-884.

23. Bodner CR, Dobson CM, Bax A (2009) Multiple tight phospholipid-binding modes of alpha-synuclein revealed by solution NMR spectroscopy. J Mol Biol 390: 775-790.
24. Fusco G, De Simone A, Gopinath T, Vostrikov V, Vendruscolo M, et al. (2014) Direct observation of the three regions in α-synuclein that determine its membrane-bound behaviour. Nat Commun 5: 3827.
25. Bodner CR, Maltsev AS, Dobson CM, Bax A (2010) Differential phospholipid binding of alpha-synuclein variants implicated in Parkinson's disease revealed by solution NMR spectroscopy. Biochemistry 49: 862-871.
26. Bussell R, Eliezer D (2004) Effects of Parkinson's disease-linked mutations on the structure of lipid-associated α-synuclein. Biochemistry 43: 4810-4818.
27. Jo E, Fuller N, Rand RP, St George-Hyslop P, Fraser PE (2002) Defective membrane interactions of familial Parkinson's disease mutant A30P alpha-synuclein. J Mol Biol 315: 799–807.
28. Volles MJ, Lee SJ, Rochet JC, Shtilerman MD, Ding TT, et al. (2001) Vesicle permeabilization by protofibrillar alpha-synuclein: implications for the pathogenesis and treatment of Parkinson's disease. Biochemistry 40: 7812-7819.
29. Clayton DF, George JM (1998) The synucleins: a family of proteins involved in synaptic function, plasticity, neurodegeneration and disease. Trends Neurosci 6: 249-254.
30. Davidson WS, Jonas A, Clayton DF, George JM (1998) Stabilization of alpha-synuclein secondary structure upon binding to synthetic membranes. J Biol Chem 273: 9443-9449.
31. Jo E, McLaurin J, Yip CM, St George-Hyslop P, Fraser PE (2000) Alpha-Synuclein membrane interactions and lipid specificity. J Biol Chem 275: 34328-34334.
32. Ueda K, Fukushima H, Masliah E, Xia Y, Iwai A, et al. (1993) Molecular cloning of cDNA encoding an unrecognized component of amyloid in Alzheimer disease. Proc Natl Acad Sci 90: 11282-11286.
33. Bertoncini CW, Jung YS, Fernandez CO, Hoyer W, Griesinger C, et al. (2005) Release of long-range tertiary interactions potentiates aggregation of natively unstructured α-synuclein. Proc Natl Acad Sci 5: 1430-1435.
34. Jao CC, Hegde BG, Chen J, Haworth IS, Langen R (2008) Structure of membrane-bound α-synuclein from site-directed spin labeling and computational refinement. Proc Natl Acad Sci 50: 19566-19571.
35. Waxman EA, Mazzulli JR, Giasson BI (2009) Characterization of hydrophobic residue requirements for alpha-synuclein fibrillization. Biochemistry 48: 9427-9436.
36. Bodles AM, Guthrie DJ, Greer B, Irvine GB (2001) Identification of the region of non-Abeta component (NAC) of Alzheimer's disease amyloid responsible for its aggregation and toxicity. J Neurochem 78: 384-395.
37. Giasson BI, Murray IV, Trojanowski JQ, Lee VMY (2001) A hydrophobic stretch of 12 amino acid residues in the middle of alpha-synuclein is essential for filament assembly. J Biol Chem 276: 2380-2386.
38. Biere AL, Wood SJ, Wypych J, Steavenson S, Jian Y, et al. (2000) Parkinson's disease associated α-synuclein is more fibrillogenic than β- and γ-synuclein and cannot cross-seed its homologs. J. Biol. Chem 275: 34574-34579.
39. Han H, Weinreb PH, Lansbury PT Jr (1995) The core Alzheimer's peptide NAC forms amyloid fibrils which seed and are seeded by beta-amyloid: Is NAC a common trigger or target in neurodegenerative disease? Chem Biol 2: 163-169.
40. ElAgnaf OM, Jakes R, Curran MD, Middleton D, Ingenito R, et al. (1998) Aggregates from mutant and wild-type alpha-synuclein proteins and NAC peptide induce apoptotic cell death in human neuroblastoma cells by formation of beta-sheet and amyloid-like filaments. FEBS Lett 440: 71-75.
41. Kahle PJ, Neumann M, Ozmen L, Muller V, Jacobsen H, et al. (2000) Subcellular localization of wild-type and Parkinson's disease-associated mutant α-synuclein in human and transgenic mouse brain. J Neurosci 20: 6365-6373.
42. Burre J, Sharma M, Tsetsenis T, Buchman V, Etherton MR, et al. (2010) Alpha-synuclein promotes SNARE-complex assembly in vivo and in vitro. Science 329: 1663-1667.
43. Li W, West N, Colla E, Pletnikova O, Troncoso JC, et al. (2005) Aggregation promoting C-terminal truncation of alpha-synuclein is a normal cellular process and is enhanced by the familial Parkinson's disease-linked mutations. Proc Natl Acad Sci USA 102: 2162-2167.
44. Liu CW, Giasson BI, Lewis KA, Lee VM, De-Martino GN, et al. (2005) A precipitating role for truncated alpha-synuclein and the proteasome in alpha-synuclein aggregation: Implications for pathogenesis of Parkinson disease. The Journal of Biological Chemistry 280: 22670-22678.
45. Hoyer W, Cherny D, Subramaniam V, Jovin TM (2004) Impact of the acidic C-terminal region comprising amino acids 109–140 on alpha-synuclein aggregation in vitro. Biochemistry 43: 16233-16242.
46. Ulusoy A, Febbraro F, Jensen P, Kirk D, Romero-Ramos M (2010) Co-experssion of C-terminal truncated alpha-synuclein enhances full-length alpha-synucleininduced pathology. European Journal of Neuroscience 32: 409-422.
47. Davies P, Moualla D, Brown DR (2011) Correction: Alpha-synuclein is a cellular ferrireductase. PLoS ONE 6: e15814.
48. Serpell LC, Berriman J, Jakes R, Goedert M, Crowther RA (2000) Fiber diffraction of synthetic alpha-synuclein filaments shows amyloid-like cross-beta conformation. Proc Natl Acad Sci USA 97: 4897-4902.
49. Crowther RA, Jakes R, Spillantini MG, Goedert M (1998) Synthetic filaments assembled from C-terminally truncated alpha-synuclein. FEBS Lett 436: 309-312.
50. Murray IV, Giasson BI, Quinn SM, Koppaka V, Axelsen PH, et al. (2003) Role of alpha-synuclein carboxy-terminus on fibril formation in vitro. Biochemistry 42: 8530-8540.
51. Burre J, Sharma M, Sudhof TC (2012) Systematic mutagenesis of α-synuclein reveals distinct sequence requirements for physiological and pathological activities. J Neurosci 32: 15227-15242.
52. Conway KA, Rochet JC, Bieganski RM, Lansbury PT Jr (2001) Kinetic stabilization of the alpha-synuclein protofibril by a dopamine-alpha-synuclein adduct. Science 294: 1346-1349.
53. Mazzulli JR, Mishizen AJ, Giasson BI, Lynch DR, Thomas SA, et al. (2006) Cytosolic catechols inhibit alpha-synuclein aggregation and facilitate the formation of intracellular soluble oligomeric intermediates. J Neurosci 26: 10068-10078.
54. Souza JM, Giasson BI, Chen Q, Lee VMY, Ischiropoulos HD (2000) Tyrosine cross-linking promotes formation of stable α-synuclein polymers. J Biol Chem 275:18344-18349.
55. Woods W, Boettcher J, Zhou D, Kloepper K, Hartman K, et al. (2007) Conformation-specific binding of alpha-synuclein to novel protein partners detected by phage display and NMR spectroscopy. J Biol Chem 282: 34555-34567.
56. Fernagut PO, Meissner WG, Biran M, Fantin M, Bassil F, et al. (2014) Age-related motor dysfunction and neuropathology in a transgenic mouse model of multiple system atrophy. Synapse 68: 98-106.
57. Tofaris GK, Razzaq A, Ghetti B, Lilley KS, Spillantini MG (2003) Ubiquitination of alpha-synuclein in Lewy bodies is a pathological event not associated with impairment of proteasome function. J Biol Chem 278: 44405-44411.
58. Mishizen-Eberz AJ, Norris EH, Giasson BI, Hodara R, Ischiropoulos H, et al. (2005) Cleavage of alpha- synuclein by calpain: potential role in degradation of fi- brillized and nitrated species of alpha-synuclein. Biochemistry 44: 7818-7829.
59. Winner B, Jappelli R, Maji SK, Desplats PA, Boyer L, et al. (2011) In vivo demonstration that alpha-synuclein oligomers are toxic. Proc Natl Acad Sci USA 108: 4194-4199.
60. Masliah E, Rockenstein E, Mante M, Crews L, Spencer B, et al. (2011) Passive immunization reduces behavioral and neuropathological deficits in an alpha-synuclein transgenic model of Lewy body disease. PLoS One 6: e19338.

61. Dufty BM, Warner LR, Hou ST, Jiang SX, Gomez-Isla T, et al. (2007) Calpain-cleavage of alpha-synuclein: connecting proteolytic processing to disease-linked aggregation. Am J Pathol 170: 1725-1738.
62. Periquet M, Fulga T, Myllykangas L, Schlossmacher MG, Feany MB (2007) Aggregated alpha-synuclein mediates dopaminergic neurotoxicity in vivo. Journal of Neuroscience 27: 3338-3346.
63. Michell AW, Tofaris GK, Gossage H, Tyers P, Spillantini MG, et al. (2007) The effect of truncated human alpha-synuclein (1–120) on dopaminergic cells in a transgenic mouse model of Parkinson's disease. Cell Transplant 16: 461-474.
64. MishizenEberz AJ, Guttmann RP, Giasson BI, Day GA 3rd, Hodara R, et al. (2003) Distinct cleavage patterns of normal and pathologic forms of alpha-synuclein by calpain I in vitro. J Neurochem 86: 836-847.
65. Tsigelny IF, Bar-On P, Sharikov Y, Crews L, Hashimoto M, et al. (2007) Dynamics of α-synuclein aggregation and inhibition of pore-like oligomer development by β-synuclein. FEBS J 274: 1862-1877.
66. Diepenbroek M, Casadei N, Esmer H, Saido TC, Takano J, et al. (2014) Overexpression of the calpain-specific inhibitor calpastatin reduces human alpha-Synuclein processing, aggregation and synaptic impairment in [A30P] alphaSyn transgenic mice. Hum Mol Genet 23: 3975-3989.
67. Games D, Valera E, Spencer B, Rockenstein E, Mante M, et al. (2014) Reducing C-terminal-truncated alpha-synuclein by immunotherapy attenuates neurodegeneration and propagation in Parkinson's disease-like models. J. Neurosci 34:9441-9454.
68. Daher JP, Ying M, Banerjee R, McDonald RS, Hahn MD, et al. (2009) Conditional transgenic mice expressing C-terminally truncated human alpha-synuclein (alphaSyn119) exhibit reduced striatal dopamine without loss of nigrostriatal pathway dopaminergic neurons. Mol Neurodegener 4: 34.
69. Tofaris GK, Garcia, Reitbock P, Humby T, Lambourne SL, et al. (2006) Pathological changes in dopaminergic nerve cells of the substantia nigra and olfactory bulb in mice transgenic for truncated human α-synuclein (1–120): Implications for Lewy body disorders. J Neurosci 26: 3942-3950.
70. Kirkwood JG (1935) Statistical mechanics of fluid mixtures. J Chem Phys 3: 300-313.
71. Duhovny D, Nussinov R, Wolfson HJ (2002) Efficient unbound docking of rigid molecules. Berlin Heidelberg Springer-Verlag 2542: 185-200.
72. Andrusier N, Nussinov R, Wolfson HJ (2007) FireDock: Fast Interaction refinement in molecular docking. Proteins 69: 139-159.
73. Laskowski RA (2001) PDBsum: Summaries and analyses of PDB structures. Nucleic Acids Research 29: 221-222.
74. Berman HM, Westbrook J, Feng Z, Gilliland G, Bhat TN, et al. (2000) The Protein data bank. Nucleic Acids Research 28: 235-242.
75. Zhang C, Vasmatzis G, Cornette JL, DeLisi C (1997) Determination of atomic desolvation energies from the structures of crystallized proteins. J Mol Biol 267: 707-726.
76. Kumar S, Bouzida D, Swendsen RH, Kollman PA, Rosenberg JM (1992) The weighted histogram analysis method for free-energy calculations on biomolecules. I. The Method. J Comput Chem 13: 1011-1021.
77. Souaille M, Roux B (2001) Extension to the weighted histogram analysis method: combining umbrella sampling with free energy calculations. Comput Phys Comm 135: 40-57.
78. Grossfield A (1995) Multidimensional free-energy calculations using the weighted histogram analysis method. J Comput Chem 16: 1339-1350.
79. Torrie GM, Valleau JP (1974) Modeling condensed phase reaction dynamics. Chem Phys Lett 28:578-s581.